ELSEVIER

Surface Science 505 (2002) 171–182

SURFACE SCIENCE

www.elsevier.com/locate/susc

Growth of thin crystalline ice films on Pt(1 1 1)

S. Haq, J. Harnett, A. Hodgson *

Surface Science Research Centre, The University of Liverpool, P.O. Box 147, Liverpool L69 3BX, UK

Received 15 November 2001; accepted for publication 7 January 2002

Abstract

Adsorption of water on Pt(1 1 1) at 135 K or above proceeds by a Stranski–Krastanov mechanism to form crystalline ice films. The structure of thin films reflects a conflict between maximising the binding to the surface and minimising the stress in the multilayer film. The first bilayer of water forms an ordered hexagonal overlayer which shows a $(\sqrt{39} \times \sqrt{39})R16.1°$ LEED pattern. Water condensation on this overlayer is initially slow, accelerating as second layer nucleation sites form and allow multilayer growth. Adsorption continues to grow the $(\sqrt{39} \times \sqrt{39})R16.1°$ structure until the film reaches a thickness of ≈ 5 bilayers at 137 K, after which further adsorption reorients the overlayer to form an incommensurate hexagonal film aligned at 30° to the Pt(1 1 1) close packed direction. Thermal desorption measurements reveal a change in the water desorption rate as the multilayer re-crystallises during heating, formation of the hexagonal $R30°$ structure stabilising the multilayer film at the cost of reducing the binding of the first layer of water to the Pt(1 1 1) surface. The $(\sqrt{39} \times \sqrt{39})R16.1°$ overlayer becomes increasingly unstable to electron exposure as its thickness increases towards five bilayers, the ice rapidly restructuring to form islands with the $R30°$ structure and exposing bare Pt. © 2002 Published by Elsevier Science B.V.

Keywords: Adsorption kinetics; Thermal desorption spectroscopy; Water; Crystallization; Platinum; Low index single crystal surfaces

1. Introduction

Water and water ice surfaces are ubiquitous in nature, playing important roles in fields as diverse as biology, atmospheric chemistry and astrophysics. In the stratosphere, reactions on ice particles in polar stratospheric clouds provide heterogeneous reaction pathways which drastically modify the halogen chemistry that leads to ozone depletion [1,2]. In some cases the reactivity of the ice surface may be dependant on its defect density or on its mobility, making it important to understand and control the structure of the ice film and the degree of crystallinity. One way to approach this problem is to grow well defined ice films on a solid surface and then to use these films to investigate atmospheric reactions [3]. In this case a good understanding of the growth mode and structure of the ice film is essential if a clear picture is to emerge of the role of the ice surface during reaction. In this paper we describe the growth of thin crystalline ice films on Pt(1 1 1) at temperatures above 135 K where adsorbed water molecules are relatively mobile. These films provide a convenient way to grow highly ordered ice films and have been used to provide surfaces on which the adsorption and reaction of atmospheric species can be studied.

* Corresponding author. Tel.: +44-151-794-3536; fax: +44-151-708-0662.

E-mail address: ahodgson@liv.ac.uk (A. Hodgson).

0039-6028/02/$ - see front matter © 2002 Published by Elsevier Science B.V.
PII: S0039-6028(02)01152-4

Water adsorbs molecularly on many close packed transition metal surfaces to form ordered, hydrogen bonded overlayers [4]. Adsorbed water is bound to metal surfaces such as Pt(1 1 1) through the O atom [5], with a binding energy that is slightly greater than that of water on an ice surface. This results in a high temperature desorption peak which can be distinguished from the multilayer ice peak which appears at higher exposures [6]. Adsorption results in ordered structures [7–9] based on the ice bilayer, consisting of units of six water molecules bound in puckered hexagonal rings. Each water molecule has hydrogen bonds to its three nearest neighbours in the other half of the bilayer, spaced 0.96 Å apart in bulk ice. Neighbouring bilayers are linked by hydrogen bonds between the adjacent layers to complete the hydrogen bonded structure, forming either hexagonal ice Ih or cubic ice Ic depending on the registry of the next nearest layers [4].

When water diffusion is suppressed by adsorption at low temperatures, water monomers are formed on the Pt(1 1 1) surface, molecules clustering to form stable dimers or trimers above 40 K [10,11]. At higher temperatures the water adsorbs in large two-dimensional ice bilayer islands [10]. If dosing is continued at temperatures below 110 K an amorphous solid water (ASW) film is formed whose morphology depends on the temperature and dosing conditions [12]. As the ASW film crystallises to form an ordered ice film there is a reduction in the vapour pressure (and hence the desorption rate) as the surface crystallises [13–15]. The crystallisation kinetics have been monitored by following variously the vapour pressure, the surface area of the film or its IR spectrum [13–16]. Crystallisation may be bulk or surface nucleated and is sensitive to the substrate [14], being particularly fast when ASW is grown epitaxially on a crystalline ice film [16].

Annealing ASW, or dosing multilayers of water at temperatures above ≈ 110 K, produces an ordered ice film with a $(\sqrt{3} \times \sqrt{3})R30°$ LEED pattern, suggesting formation of an epitaxial layer of ice [6–8]. LEED IV measurements of ice films grown on this surface show that the film is hexagonal ice Ih, the surface being terminated with a complete unreconstructed (0 0 0 1) bilayer in which the top layer has an unusually large vibrational amplitude [17,18]. Recent He atom scattering measurements confirm that the surface terminates in a (1×1) overlayer with the bulk ice spacing [19]. This spacing is some 6% greater than the Pt repeat distance, $\sqrt{3}a_0$, the overlayer being incommensurate with the Pt (1 1 1) surface.

The structure adopted by ice films on different hexagonal metal surfaces is sensitive to the binding energy to the metal and to the mismatch between the metal lattice and the spacing of the ideal hydrogen bonded water bilayer, different structures forming on different transition metal surfaces [4]. Adsorption on Ru(0 0 0 1) has been studied in detail, D_2O adsorbing on top of Ru atoms to form a commensurate $(\sqrt{3} \times \sqrt{3})R30°$ structure with a compression of the bilayers perpendicular to the surface which helps to stabilise the water dipole–dipole interaction [20]. Unusually, this surface shows a structural isotope effect, H_2O films forming stripes with periodic domain boundaries [21]. Similar hexagonal structures with periodic antiphase domain boundaries have been observed on other hexagonal surfaces [4]. The domain boundaries in these structures act to relieve stress in the ice lattice, allowing water to bind in favourable surface sites while maintaining maximum hydrogen bonding in the ice film.

STM studies on Pt(1 1 1) showed several ordered phases based around the hexagonal ice bilayer unit but with differing superstructures and densities [22]. He atom scattering found two different ordered ice structures during growth of the first bilayer, islands of a $(\sqrt{37} \times \sqrt{37})R25.3°$ structure forming at sub-bilayer coverage followed by a $(\sqrt{39} \times \sqrt{39})R16.1°$ structure on completion of the first water bilayer [23]. These structures have slightly different densities, the $\sqrt{37}$ islands having a 4% expansion and the saturation $\sqrt{39}$ bilayer a 3% compression compared to a bulk ice bilayer. Stress in the ice layer can be relieved by relaxing the bilayer spacing perpendicular to the film, allowing the water molecules to retain their preferred H-bonding separation [23].

Water molecules prefer to bind to the Pt(1 1 1) surface via the O atom [5,6,24], suggesting that the lower half of the first ice bilayer will consist of water with the OH bonds pointing towards the

O atoms in the upper bilayer. In order to obtain a fully H-bonded bilayer and still obey the Bernal–Fowler–Pauling rules, water in the upper half of the bilayer must have one H atom aligned towards the second bilayer [25]. This creates a structure where each successive bilayer is forced into the same orientation, the proton order transferring up through the film, in contrast to bulk ice which is proton disordered. Each water molecule in the top layer will then have a dangling OH group pointing out of the surface, an arrangement that might be expected to cause reconstruction of the surface to satisfy some of the hydrogen bonds [26,27]. LEED [17,18] and He atom scattering both indicate a (1×1) termination for thin films grown on Pt(1 1 1) but could not determine the proton ordering of these films [28]. Evidence for some proton ordering has been seen using sum-frequency generation [29], but the degree of orientational ordering was not determined and the absence of large shifts in work function suggests that this may be small, thick ice films grown on Pt(1 1 1) showing only a weak bulk proton ordering favouring O at the surface [30]. Recently Witek and Buch [31] have carried out simulations to look at the influence of the water orientation and flattening of the first bilayer in contact with the metal surface [20] on the structure of thin ice films on metal surfaces. They find that when the first layer is flattened perpendicular to the surface the ice preferred to adopt a ''sandwich'' structure, in which subsequent bilayers pair their dangling OH groups to give an odd-even alternation in the surface properties with thickness. For models based on a puckered first layer, the proton ordering was found to decay over a length scale of just 2–3 bilayers (BL) via a defect mechanism which created dangling OH groups pointing into the ice film [31].

Here we describe the growth of thin crystalline ice films on Pt(1 1 1) at temperatures above 135 K where adsorbed water molecules are relatively mobile. Using molecular beam adsorption, LEED and TPD we show how water adsorption and the structure of the film changes with thickness. Slow growth of ice on Pt(1 1 1) produces a bilayer which shows a sharp $(\sqrt{39} \times \sqrt{39})R16.1°$ LEED pattern. As adsorption on this surface continues the $(\sqrt{39} \times \sqrt{39})R16.1°$ structure becomes metastable with respect to a hexagonal $R30°$ overlayer, the film restructuring when around four to five bilayers thick at 137 K to form a hexagonal $(\sqrt{3} \times \sqrt{3})R30°$ structure characteristic of bulk ice films. RAIR spectra remain unchanged by reordering of the film and we found no evidence for the formation of additional dangling OH groups in the lattice or of more complex 'sandwich' type structures. The thin $(\sqrt{39} \times \sqrt{39})R16.1°$ ice films are also unstable under electron exposure, the film restructuring to form islands of the hexagonal $\sqrt{3}$ structure and bare Pt.

2. Experimental

Experiments were conducted in a UHV chamber with a base pressure of 3×10^{-11} mbar. The Pt(1 1 1) crystal was cleaned by a conventional Ar^+ ion sputtering and annealing procedure, the cleanliness being checked by LEED and thermal desorption spectroscopy. The crystal was spot welded to two Ta heating wires which were attached to high current feed-throughs mounted in the base of a liquid nitrogen cooled manipulator. Temperature was measured by a chromel–alumel thermocouple spot welded to the crystal. This arrangement allowed the crystal to be heated or cooled rapidly, with minimal desorption from the support and, when combined with molecular beam dosing, provided clean temperature programmed desorption (TPD) spectra free from edge or support effects. The structure of the ice film was characterised using a combination of LEED (VG) and reflection absorption infrared spectroscopy (RAIRS) using a Mattson 6020 FTIR spectrometer with 4 cm^{-1} resolution.

Water was dosed on to the surface using an effusive, low pressure molecular beam, with two stages of differential pumping, to form a 5 mm diameter spot on the surface. Sticking probabilities were determined using the direct reflection technique of King and Wells [32]. A flag in the main chamber prevented the beam hitting the surface until desired. The partial pressure of water in the chamber was measured using a quadrupole mass spectrometer (VG micromass) and the fraction of the incident molecular beam that adsorbs

determined from the decrease in partial pressure as the beam was allowed to strike the surface. This technique provides absolute sticking probabilities with an accuracy of $\approx\pm 0.03$ and a similar lower limit on the values of S which can be measured. The coverage dependence $S(\Theta)$ was determined from the time behaviour of the uptake traces. These were converted to an absolute scale by using the TPD spectra to establish the uptake of water on the surface. The TPD profile for the first bilayer of water on Pt(1 1 1) is well separated from the ice multilayer peak [6], allowing the total water uptake to be calibrated relative to the coverage of the first bilayer. All water coverages are referenced to the density of water in an ideal hexagonal $(\sqrt{39} \times \sqrt{39})R16.1°$ bilayer (1 BL $= 1.2 \times 10^{15}$ cm^{-2}).

3. Results

Crystalline ice films were grown by exposing the Pt(1 1 1) surface to a thermal molecular beam of water with the surface held at 137 K. LEED measurements, which are described in more detail below, showed that the quality of the crystalline ice films produced was sensitive to the growth rate and the surface temperature. Sharp LEED patterns and well ordered ice films resulted from slow growth rates (typically around 0.01 BL s^{-1} for the films described here) and high adsorption temperatures, $T \geqslant 135$ K. This ensured that water molecules trapping on to the ice surface were mobile, able to diffuse across the surface and to desorb if they do not find a favourable binding site. Similar conditions were used by Toennies and co-workers to obtain well ordered crystalline overlayers which showed strong He diffraction peaks [19,23,28].

The resulting crystalline ice films (1–100 BL thick) showed a simple two peak structure during thermal desorption, Fig. 1a, very similar to that reported by Fisher and Gland [6]. The first peak near 168 K saturates with exposure and is due to the first bilayer of water adsorbed directly on the Pt(1 1 1) surface. For sub-bilayer coverages, where the surface consists of islands of a water bilayer [23,33], the desorption peak shape indicates fractional order kinetics, intermediate between the zero order kinetics of a bulk film and the first order

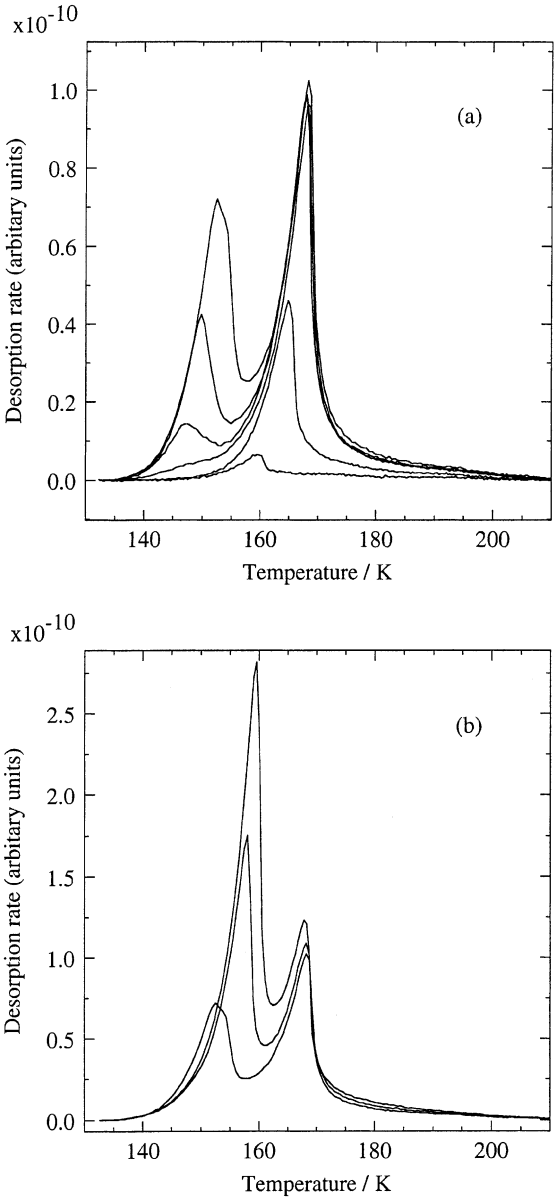

Fig. 1. Desorption of water from Pt(1 1 1) after growth of a crystalline ice film at 137 K, taken with a heating rate of 0.65 Ks^{-1}. (a) Desorption of water from a $(\sqrt{39} \times \sqrt{39})R16.1°$ ice film showing the first bilayer peak at 168 K and the development of the multilayer peak for initial coverages of 0.1, 0.45, 1.0, 1.14, 1.3 and 1.7 BL. (b) Shift in the position of the multilayer peak at higher coverages (1.7, 2.3 and 3.2 BL).

behaviour that might be expected for desorption of islands from a flat surface. Since the binding energy of water to Pt(1 1 1) is comparable to that in the water bilayer, desorption is expected to originate from molecules which have a reduced degree of hydrogen bonding, for example those adsorbed at island edges. Fractional order and pseudo-zero order kinetics can occur when a reservoir of adsorbate supplies a dilute phase which acts as a precursor to desorption [34], and has been seen for water desorption in other systems [4,6].

After continued water exposure at 137 K a multilayer peak appears near 155 K, Fig. 1a, which does not saturate even after extended exposures. Initially this peak shows a common leading edge but with increasing uptake the peak shows a small but systematic shift to higher temperature, Fig. 1b. Continued exposure to grow films >3 BL thick results in a large zero order desorption peak which eventually obscures the surface peak. The small shift in the desorption peak for initial coverages between 2 and 4 BL is associated with re-crystallisation of the ice film during heating and is discussed in more detail below.

Two additional desorption features have been reported in previous studies on Pt(1 1 1), neither of which we observed here. Jo et al. [35] reported a splitting of the bilayer desorption peak which they attributed to the two different water species in the bilayer. The stability of the bilayer is too dependant on the H-bonded structure to expect separate desorption features for molecules from the upper and lower layers and no similar splitting was observed here for crystalline ice films. The population depended on the adsorption temperature, 55 or 110 K [35], suggesting they were probably related to ordering of the initial ASW film during heating. Some studies have observed an additional peak near 190 K [24], which again we do not see, although we do find a tail extending out to ~200 K during desorption from thicker ice films, Fig. 1. The high temperature peak has been attributed to water monomers on the Pt surface [24], although it seems unlikely that loss of the hydrogen bonding structure would make isolated water molecules more stable. Morgenstern et al. [22] showed that rows of water atoms remain bound at Pt step sites even after the terrace bilayer has desorbed and suggested that this may be responsible for the water desorption in this region. We find that this high temperature TPD feature is not visible on a freshly prepared surface. Desorption in this region can be enhanced by roughening of the surface but a clear peak near 200 K developed only when the surface was dosed with oxygen, supporting the idea that this originates from OH recombination when water is adsorbed on O atoms [6,35,36].

At low temperature ($T < 135$ K) water adsorption on to the Pt(1 1 1) surface occurs with a sticking probability which is unity within experimental error, Fig. 2, slightly larger than the 0.7 [37] estimated previously. Subsequent film growth to form amorphous solid water (ASW) continues with unit sticking probability at $T < 135$ K. This is consistent with recent beam measurements of water condensation on ice films by Smith and Kay [15,38], efficient energy exchange and trapping at the surface being expected in view of the large amplitude phonon modes of the ice surface [19]. The sticking probability on the Pt(1 1 1) surface remains unchanged up to ≈ 150 K, but above 135 K water desorption from multilayer ice begins to compete with adsorption, resulting in a net sticking probability which is dependant on both film temperature and the water flux (Fig. 2). In this regime the sticking probability is more properly called a condensation coefficient, representing the difference between the rate at which water is adsorbed from the beam (with a unit trapping probability) and the desorption rate which is determined by the surface temperature [15].

Around 144.3 K adsorption of further water on top of the first layer is balanced by desorption, Fig. 2a, and water uptake terminates with formation of a single bilayer of water on the Pt(1 1 1) surface, Fig. 1. At slightly lower temperatures the sticking probability (or condensation coefficient) drops as the bilayer is completed but then recovers slightly to stabilise with S somewhere between 0 and 1. Water adsorption from the beam and thermal desorption from the ice film compete and the film grows at a constant rate, determined by the beam flux and surface temperature. As film growth continues we do not see any further abrupt changes in the sticking probability which might correspond to completion of a second or third bilayer of

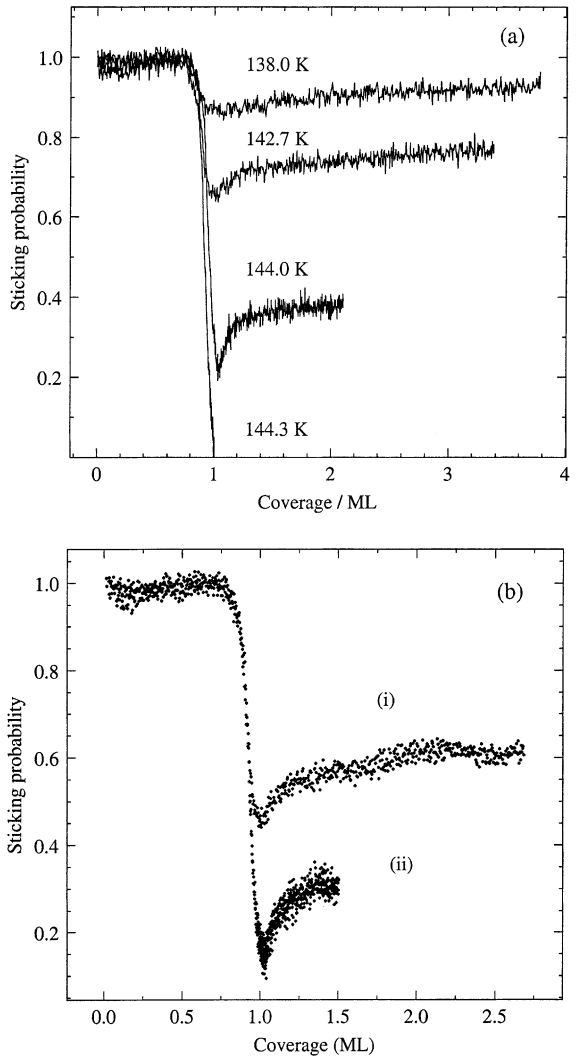

Fig. 2. Adsorption of water on the Pt(1 1 1) surface as a function of (a) the surface temperature and (b) the flux of water, (i) 3.7×10^{-3} and (ii) 6.6×10^{-3} BL s^{-1} respectively, at 143 K.

ice, indicating that the ice film grows by a Stranski–Krastanov mechanism to form a three dimensional ice after the first bilayer is complete.

The minimum in the water sticking probability (condensation coefficient) as the surface bilayer is completed is followed by a recovery as the multilayer film starts to grow. The majority of this recovery is complete by the time a further 0.2 BL of water has adsorbed on the first ice bilayer, although the condensation rate continues to increase slowly as the first few layers of water condense, Fig. 2. Assuming that water continues to trap efficiently on the ice surface, the recovery in S as the multilayer film grows indicates that water adsorption on top of the first bilayer is kinetically unfavourable. The water desorption rate increases to a maximum just after the first bilayer of ice has covered the surface, but drops as the multilayer ice film starts to grow. This behaviour indicates that multilayer formation requires water clusters or islands to nucleate on the first bilayer before adsorption can proceed efficiently. Water molecules trapping on to terraces of the completed Pt(1 1 1)/ice bilayer water can hydrogen bond only to water molecules in the underlying layer, resulting in a weakly bound species which will be mobile on the surface and has a lower desorption energy than molecules fully incorporated into a surface bilayer. Isolated water molecules on the bilayer terraces stabilise themselves by clustering to form ice Ih nuclei, providing step edge sites which act as favourable binding sites for subsequent water adsorption. As the ice nuclei form, the chances of a water molecule trapping on the surface and finding a favourable binding site before desorption increase, leading to an increase in growth rate with coverage. This picture is consistent with STM observations of ice growth on Pt(1 1 1) where second layer water was found to nucleate homogeneously on the bilayer terraces [22], rather than at step sites. The adsorption data (Fig. 2) indicate that sufficient nuclei have formed by the time 0.2 BL water has adsorbed on the Pt(1 1 1)/ice bilayer for diffusion to enable most trapped molecules to find favourable adsorption sites before desorbing, but a slow increase in the adsorption rate continues as the first few ice layers grow, indicating a continuing increase in ice step density. We did not observe any further minima in the growth rate which might correspond to completion of the second or subsequent ice bilayers, the ice multilayer growing by three dimensional growth with a relatively high rate of island nucleation. This is consistent with He scattering where no intensity oscillations were observed which might indicate layer by layer growth [28].

Growth of crystalline ice films on the Pt(1 1 1) surface was monitored using LEED to probe the

ordering of the films and their registry to the Pt surface. The ice films are unstable under the action of the electron beam and the LEED patterns change on a timescale that is dependant on the film thickness and the ice structure, this is discussed further below. When the ice films were grown slowly, typically 0.01 BL s^{-1} at temperatures about 137 K, sharp LEED patterns were observed when the film was cooled to 85 K and first exposed to the LEED beam. Increasing the growth rate or lowering the surface temperature both reduced the quality of the LEED patterns. Rapid growth of the films prevents partially hydrogen bonded molecules in the surface diffusing to a favourable site or desorbing before being incorporated into the growing film, reducing the quality of the film [23,28]. Similar LEED patterns and behaviour were observed for both H_2O and D_2O, consistent with the absence of any Ubbelohde effect on Pt(1 1 1). The LEED patterns primarily reflect the positions of the O atoms in the overlayer [18] and it was noticeable that D_2O films showed more intense ice patterns, presumably the result of the reduced zero-point motion of the deuterated film.

Completion of the ice bilayer on Pt(1 1 1) gave rise to a sharp $(\sqrt{39} \times \sqrt{39})R16.1°$LEED pattern, Fig. 3a,b. This is in agreement with recent He atom scattering measurements which show formation of a $(\sqrt{39} \times \sqrt{39})R16.1°$ water overlayer at saturation under similar growth conditions [23,28]. This overlayer has the hexagonal bilayer structure but with a water density which is some 3% greater than that of an ideal bulk ice layer [23], maximising the amount of water bound directly to the Pt surface at the expense of some distortion of the water away from its preferred hydrogen bonding

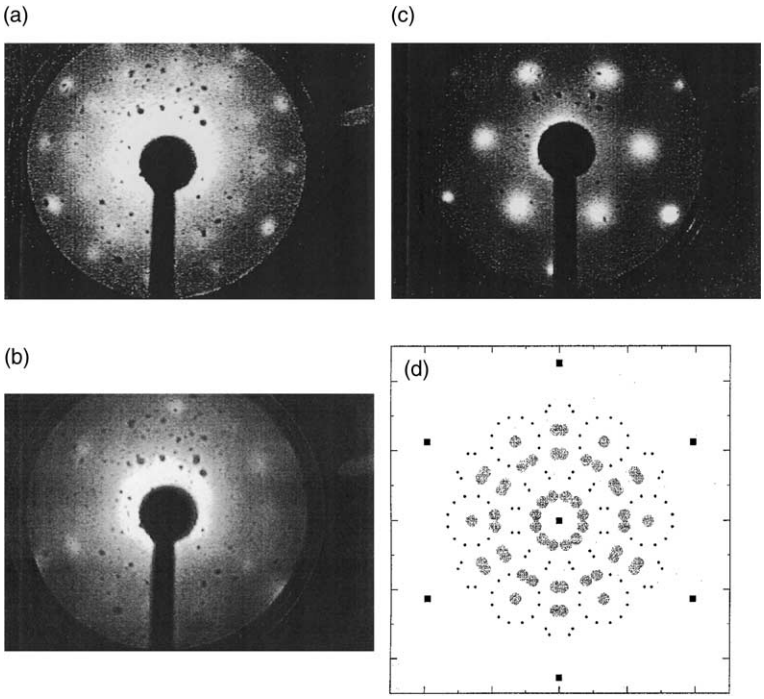

Fig. 3. LEED patterns obtained at 90 K after dosing the Pt(1 1 1) surface with D_2O at 137 K. (a) and (b) show the LEED pattern obtained at low energy (23 and 19 V respectively) for diffraction from a complete D_2O ice bilayer with the $(\sqrt{39} \times \sqrt{39})R16.1°$ spots visible as three rings inside the Pt(1 1 1) spots (not shown). (c) LEED pattern ($E = 56$ eV) of D_2O on Pt(1 1 1) after exposure to electrons from the LEED gun, showing the Pt(1 1 1) spots (outer ring) and the $(\sqrt{3} \times \sqrt{3})R30°$ spots due to islands of hexagonal ice. (d) Schematic representation of the reciprocal lattice vectors of the $(\sqrt{39} \times \sqrt{39})R16.1°$ bilayer on Pt(1 1 1) showing the Pt substrate as black squares with the overlayer spots visible in (a) and (b) indicated as circles.

geometry. For water coverages below saturation we did not observe an ordered LEED pattern even when the film was cooled to 85 K, just an increase in the diffuse background intensity. In contrast He scattering indicated islands of a $(\sqrt{37} \times \sqrt{37})$ $R25.3°$ structure formed at low coverage during growth of the first water bilayer [23]. Continued adsorption of water on the $(\sqrt{39} \times \sqrt{39})R16.1°$ overlayer resulted in adsorption of a total of 4–5 BL of ice without any change in the LEED pattern. Further film growth resulted in a change of behaviour, the $(\sqrt{39} \times \sqrt{39})R16.1°$ pattern disappearing to be replaced by the hexagonal $R30°$ pattern observed for thicker films, Fig. 3c. The diffuse nature of the $R30°$ ice spots made it impossible to distinguish whether this structure was in registry with the Pt surface, forming a $(\sqrt{3} \times \sqrt{3})R30°$ overlayer, but He atom scattering [28] and LEED-IV [18] measurements indicate that the hexagonal ice surface has the ideal bulk truncation with a lattice spacing identical to that of bulk ice Ih (6% greater than the Pt repeat distance, $\sqrt{3}a_0$). This LEED pattern could be seen for films up to around 50 BL or so thick, as the Pt(1 1 1) spots disappear from view.

As water was adsorbed on the $(\sqrt{39} \times \sqrt{39})$ $R16.1°$ overlayer it became increasingly unstable to electrons from the LEED beam. Whereas the LEED pattern of the first bilayer was stable for ~1 min under electron exposure, by the time the film was 5 BL thick the pattern disappeared in a few seconds, to be replaced by the hexagonal $R30°$ pattern characteristic of thicker ice multilayer films. No water desorption was observed under the action of the LEED beam, indicating that the ice film restructures rather than desorbing from the surface. In order to see if this created vacant Pt sites we measured the sticking probability of CO on the $(\sqrt{39} \times \sqrt{39})R16.1°$ overlayer and compared this to sticking on the film which has been annealed by electron exposure to form the hexagonal $R30°$ film. The sticking probability of CO on the bare Pt(1 1 1) surface was (0.63 ± 0.02), as expected [39], while on 2 BL of the $(\sqrt{39} \times \sqrt{39})$ $R16.1°$ ice S was zero within our experimental error (2%). The sticking probability for CO on the first bilayer of ice was found to be (0.1 ± 0.02), probably the result of CO incorporating into the water film to form coadsorbate structures [40–42]. Once the first $(\sqrt{39} \times \sqrt{39})R16.1°$ bilayer had been restructured to form the hexagonal $R30°$ ice structure by exposure to the electron beam, the CO sticking probability increased to (0.4 ± 0.02). This is consistent with the formation of three dimensional islands of hexagonal ice on the surface, exposing approximately 2/3 of the Pt surface.

Restructuring of the ice film can be correlated with changes in the desorption rate of water during heating, Fig. 1. The first bilayer of water adsorbed directly on to the Pt(1 1 1) surface desorbs near 168 K with an activation barrier of 52 ± 2 kJ mol^{-1}. Further dosing results in the growth of ice multilayers which retain the $(\sqrt{39} \times \sqrt{39})R16.1°$ structure. For coverages between 1 and 2 BL desorption starts near 135 K, the TPD curves displaying a common leading edge, indicating zero order behaviour, with the desorption peak shifting up from 147 to 153 K as the initial coverage increases to 2 BL. The activation energy obtained from the leading edge of these TPD curves is 50 ± 2 kJ mol^{-1}, identical to the heat of sublimation of water [43]. For ice films thicker than 2 BL the leading edge of the desorption curves shifts to higher temperature, Fig. 1, and the apparent activation energy changes. For ice films below 4 or 5 BL thick the leading edge of the desorption peaks no longer coincide, indicating kinetics which are intermediate between zero and first order. Only when the film thickness is increased above 5 BL or so is the zero order leading edge regained with the same activation energy. When the heating ramp is interrupted and the surface cooled we find that multilayer films with the $(\sqrt{39} \times \sqrt{39})R16.1°$ structure have reconstructed to the hexagonal $R30°$ pattern associated with the growth of thick ice films, so reducing the water desorption rate. The $(\sqrt{39} \times \sqrt{39})R16.1°$ structure was only observed during growth of water films and was never observed when thicker layers with the $R30°$ structure were allowed to partially desorb to form thin films.

The RAIR spectrum of thin ice films was examined in order to look for evidence for formation of distinguishable structures [31] and changes associated with the reconstruction of films >5 BL. Both H_2O and D_2O films showed identical behaviour and spectra taken during growth of a D_2O

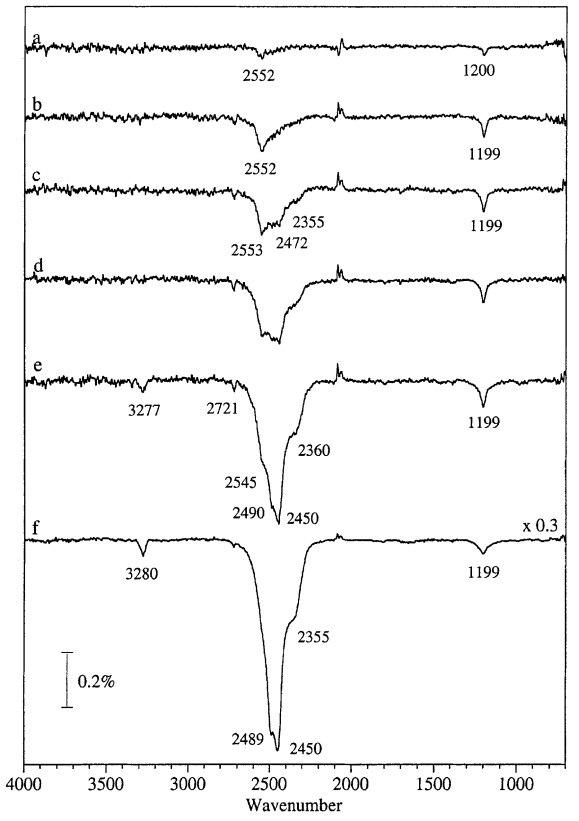

Fig. 4. RAIR spectra for thin films of D_2O ice grown on Pt(1 1 1). (a)–(e) $(\sqrt{39} \times \sqrt{39})R16.1°$ films of thickness 0.2, 0.6, 0.9, 1.1 and 1.4 BL respectively. (f) 7 BL ice layer showing a $(\sqrt{3} \times \sqrt{3})R30°$ LEED pattern. The band near 3280 cm^{-1} is due to impurity H_2O.

film at 140 K are shown in Fig. 4 for convenient comparison with the IR spectra reported by Ogasawara et al. [11,24]. For sub-bilayer coverages two bands appear, at 2552 cm^{-1} (OD stretch) and 1199 cm^{-1} (bend), with a strong band at 2472 cm^{-1} and a weaker shoulder near 2355 cm^{-1} appearing as the coverage increases towards saturation of the $(\sqrt{39} \times \sqrt{39})R16.1°$ bilayer. At the same time a weak band due to the free OD stretch appears at 2721 cm^{-1} [44]. This band is shifted compared to the 2706 cm^{-1} observed for a monomer on Pt(1 1 1) [11] and is associated with the uncoordinated OD in the upper half of the bilayer. As expected, we did not see sharp bands due to monomer or dimer adsorption at 137 K [11], consistent with the formation of islands of hydrogen bonded ice even at the lowest exposures. The 2552 and 1199 cm^{-1} bands formed at low coverages are identical to those seen during annealing of sub-bilayer films to 125 K [11] and are associated with the presence of amorphous ice on the surface above its melting temperature. We did not see an ordered LEED pattern when the low coverage surface was cooled, although ordered islands were seen by He atom scattering [23]. The 2552, 2472 and 1199 cm^{-1} bands are similar to those seen after deposition of a 1 BL film at 84 K [24].

As a second bilayer grows the spectrum becomes dominated by the stretching bands at 2355, 2450 and 2489 cm^{-1} associated with an ordered ice film. These bands continue to grow as the film develops. Once the first bilayer is complete the free OD band at 2721 cm^{-1} remains unchanged in size (±25%) as the thickness of the ice films increases, whereas this band continues to grow in intensity during formation of ASW at low temperature as defect sites with uncoordinated OD groups are introduced into the surface. This indicates that the number of free OD groups is unchanged after the first bilayer is formed, again consistent with a crystalline structure and (1×1) termination of the surface. As the $(\sqrt{39} \times \sqrt{39})R16.1°$ structure relaxes to form the $R30°$ overlayer we can see no change in either the frequency of the stretching bands near 2400–2500 cm^{-1} or the intensity of the free OD band.

4. Discussion

Water adsorption on to Pt(1 1 1) occurs with unit sticking probability at temperatures below 145 K, He atom diffraction measurements showing islands of a $(\sqrt{37} \times \sqrt{37})R25.3°$ structure [23] which we do not see by LEED. As the surface saturates a $(\sqrt{39} \times \sqrt{39})R16.1°$ bilayer forms which shows a well ordered LEED pattern. This film has a water density 3% greater than that of an ideal ice bilayer, the additional water—Pt binding stabilising some distortion of the bilayer away from the ideal hydrogen bonded geometry. Desorption occurs as a single peak near 168 K, probably from a liquid phase [11,22]. As water is

dosed onto this surface the $(\sqrt{39} \times \sqrt{39})R16.1°$ bilayer acts as a template on which the second and subsequent multilayers of ice grow. Initially water molecules which trap onto the bilayer terraces are unable to find favourable second layer sites where they can form a hydrogen bonded network and desorption competes effectively with diffusion across the surface to create second layer ice nuclei [22]. As the coverage increases the chances of finding a suitable binding site, such as a step or kink site, before the trapped molecule desorbs increases and the condensation rate recovers, Fig. 2.

As the $(\sqrt{39} \times \sqrt{39})R16.1°$ ice film grows thicker, the stress associated with the lateral compression destabilises the film. At some point the strain energy will outweigh the stabilisation gained from the additional water—Pt binding in the first bilayer and the structure becomes unstable with respect to formation of a bulk ice film. Although the top most ice bilayer is rather mobile, lower bilayers are rigidly held by the H-bonding structure [45] and continued adsorption on this film may produce a metastable structure. Ice layers grown at 137 K retain the $(\sqrt{39} \times \sqrt{39})R16.1°$ LEED pattern of the underlying ice template up to ca 5 BL thickness. Continued growth restructures the film to form a hexagonal 30° overlayer, with relatively diffuse LEED spots near the $(\sqrt{3} \times \sqrt{3})$-$R30°$ positions. These overlayers show Pt(1 1 1) spots but no trace of the original $(\sqrt{39} \times \sqrt{39})$-$R16.1°$ pattern, indicating that the entire film, including the lowest layers, has reordered to form the bulk hexagonal ice structure. This rearrangement is not reversible, desorbing water from the hexagonal $R30°$ film does not form a $(\sqrt{39} \times \sqrt{39})$-$R16.1°$ overlayer. Although formation of the hexagonal $R30°$ structure reduces the number of water molecules tightly bound in contact with the Pt(1 1 1) surface, this is compensated by a reduction in the strain energy of the multilayers.

Restructuring of the $(\sqrt{39} \times \sqrt{39})R16.1°$ film can also be induced by heating the film above 140 K or by electrons from the LEED gun. Heating 3–5 BL ice films during TPD results in a shift in the desorption curves to higher temperature, indicating a reduction in the desorption rate. This shift may be due either to a reduction in the vapour pressure of the ice as it relaxes to the bulk ice structure, or to a change in surface area of the ice multilayer as the film clusters on the surface. This behaviour suggests that even thin $(\sqrt{39} \times \sqrt{39})$-$R16.1°$ multilayer films grown at 137 K are metastable. Thicker films, where the overlayer has already relaxed to the $\sqrt{3}$ $R30°$ structure, show simple zero order desorption kinetics.

Under electron exposure even the 85 K bilayer film slowly reverts to the bulk ice structure, at the cost of exposing bare Pt. This process becomes increasingly rapid as the $(\sqrt{39} \times \sqrt{39})R16.1°$ film gets thicker. Chakarov and Kasemo [46] have observed electron induced clustering and crystallisation of water on graphite following exposure to UV radiation. This was attributed to injection of electrons into the conduction band, followed by trapping to create negative ion states which 'annealed' the film and increased the local water coordination. We believe a similar mechanism may be operating in the case of Pt(1 1 1), although in this case the initial overlayer is highly crystalline rather than amorphous. In the case of graphite there was a reduction in the crystallisation rate with thickness which was attributed to the tunnelling length of the electrons, whereas we find an increase in the rate of reconstruction for thicker films on Pt(1 1 1). This suggests that the increased strain energy of the $(\sqrt{39} \times \sqrt{39})R16.1°$ film assists electron induced re-crystallisation as the ice film gets thicker. However this process cannot be described simply as annealing, since electron stimulated restructuring of the first bilayer does not form the minimum energy structure. The increased binding energy of water to Pt and the mobility of water during growth of the bilayer structure both suggest that the $(\sqrt{39} \times \sqrt{39})R16.1°$ bilayer is the minimum energy structure. Clustering of this first layer is more akin to electron induced damage to the original film, some water molecules being displaced and initiating nucleation of small clusters of the bulk ice structure leaving some of the Pt(1 1 1) surface bare.

In addition to the lateral compression of the $(\sqrt{39} \times \sqrt{39})R16.1°$ bilayer, thin water films may be proton ordered. Using simulations of thin ice layers on a metal surface Witek and Buch [31] have

suggested a defect mechanism for decay of the proton ordering over a length scale of just 2–3 BL. Both the lateral compression of the $(\sqrt{39} \times \sqrt{39})$-$R16.1°$ bilayer and alignment of the water dipole moments induced by Pt–O bonding at the surface will contribute to the stress in thicker multilayers grown on this template. It therefore seems likely that both the lateral compression and the orientational ordering will be lost as the film relaxes to the bulk geometry associated with the $R30°$ structure. Disruption of the water dipole orientation might also help to explain why electron attachment is so efficient in restructuring thicker $(\sqrt{39} \times \sqrt{39})R16.1°$ films. The IR spectra do not show any change as the film reconstructs to the bulk ice structure. In particular we do not see evidence for a significant increase in the density of uncoordinated OD groups in the film, indicating that reconstruction of the film, and any loss of proton ordering which may occur, is not associated with a significant change in the overall crystallinity of the film. Orientational order may be lost by the creation of internal dangling OD bonds [31] but since these are likely to show a similar frequency to the surface group this would not be discernible in the IR spectrum.

5. Conclusions

Water adsorbs on Pt(1 1 1) at temperatures between 135 and 145 K to form an ordered hexagonal bilayer with a $(\sqrt{39} \times \sqrt{39})R16.1°$ structure. Further growth on this surface proceeds via a Stranski–Krastanov mechanism, second layer ice nucleating on the bilayer terraces to form stable sites for further water adsorption. The first bilayer acts as a template for crystallisation of further water, producing a metastable film up to 5 BL thick at 137 K. Further adsorption results in restructuring of the film to form the hexagonal $R30°$ overlayer characteristic of bulk ice, so removing the stress induced in the bulk ice film by the lateral compression of the initial bilayer on Pt(1 1 1). The metastable film is converted to the bulk ice phase by exposure to low energy electrons, which induce clustering in the film and expose bare Pt.

References

[1] M.J. Molina, T.L. Tso, L.T. Molina, F.C.Y. Wang, Science 238 (1987) 1253.
[2] M.J. Rossi, R. Malhotra, D.M. Golden, Geophys. Res. Lett. 14 (1987) 127.
[3] S.M. George, F.E. Livingston, Surf. Rev. Lett. 4 (1997) 771.
[4] P.A. Thiel, T.E. Madey, Surf. Sci. Rep. 7 (1987) 211.
[5] B.A. Sexton, Surf. Sci. 94 (1980) 435.
[6] G.B. Fisher, J.L. Gland, Surf. Sci. 94 (1980) 446.
[7] L.E. Firment, G.A. Somorjai, J. Chem. Phys. 63 (1975) 1037.
[8] L.E. Firment, G.A. Somorjai, Surf. Sci. 84 (1979) 275.
[9] U. Starke, K. Heinz, N. Materer, A. Wander, M. Michl, R. Doll, M.A. van Hove, G.A. Somorjai, J. Vac. Sci. Tech. A 10 (1992) 2521.
[10] A.L. Glebov, A.P. Graham, A. Menzel, Surf. Sci. 428 (1999) 22.
[11] H. Ogasawara, J. Yoshinobu, M. Kawai, J. Chem. Phys. 111 (1999) 7003.
[12] K.P. Stevenson, G.A. Kimmel, Z. Dohnalek, R.S. Smith, B.D. Kay, Science 283 (1999) 1505.
[13] R.S. Smith, C. Huang, E.K.L. Wong, B.D. Kay, Surf. Sci. 367 (1996) L13.
[14] P. Lofgren, P. Ahlstrom, D.V. Chakarov, J. Lausmaa, B. Kasemo, Surf. Sci. 367 (1996) L19.
[15] R.S. Smith, B.D. Kay, Surf. Rev. Lett. 4 (1997) 781.
[16] Z. Dohnalek, R.L. Ciolli, G.A. Kimmel, K.P. Stevenson, R.S. Smith, B.D. Kay, J. Chem. Phys. 110 (1999) 5489.
[17] N. Materer, U. Starke, A. Barbieri, M.A. Vanhove, G.A. Somorjai, G.J. Kroes, C. Minot, J. Phys. Chem. 99 (1995) 6267.
[18] N. Materer, U. Starke, A. Barbieri, M.A. VanHove, G.A. Somorjai, G.J. Kroes, C. Minot, Surf. Sci. 381 (1997) 190.
[19] J. Braun, A. Glebov, A.P. Graham, A. Menzel, J.P. Toennies, Phys. Rev. Lett. 80 (1998) 2638.
[20] G. Held, D. Menzel, Surf. Sci. 316 (1994) 92.
[21] G. Held, D. Menzel, Phys. Rev. Lett. 74 (1995) 4221.
[22] M. Morgenstern, J. Muller, T. Michely, G. Comsa, Z. Phys. Chem. 198 (1997) 43.
[23] A. Glebov, A.P. Graham, A. Menzel, J.P. Toennies, J. Chem. Phys. 106 (1997) 9382.
[24] H. Ogasawara, J. Yoshinobu, M. Kawai, Chem. Phys. Lett. 231 (1994) 188.
[25] D.L. Doering, T.E. Madey, Surf. Sci. 123 (1982) 305.
[26] J.P. Devlin, C. Joyce, V. Buch, J. Phys. Chem. A 104 (2000) 1974.
[27] J.P. Devlin, V. Buch, Mikrochimica Acta (1997) 57.
[28] A. Glebov, A.P. Graham, A. Menzel, J.P. Toennies, P. Senet, J. Chem. Phys. 112 (2000) 11011.
[29] X.C. Su, L. Lianos, Y.R. Shen, G.A. Somorjai, Phys. Rev. Lett. 80 (1998) 1533.
[30] M.J. Iedema, M.J. Dresser, D.L. Doering, J.B. Rowland, W.P. Hess, A.A. Tsekouras, J.P. Cowin, J. Phys. Chem. B 102 (1998) 9203.
[31] H. Witek, V. Buch, J. Chem. Phys. 110 (1999) 3168.

[32] D.A. King, M.G. Wells, Surf. Sci. 29 (1972) 454.
[33] M. Morgenstern, T. Michely, G. Comsa, Phys. Rev. Lett. 77 (1996) 703.
[34] H.J. Kreuzer, S.H. Payne, Studies Surf. Sci. Catal. 104 (1997) 153.
[35] S.K. Jo, J. Kiss, J.A. Polanco, J.M. White, Surf. Sci. 253 (1991) 233.
[36] F.T. Wagner, T.E. Moylan, Surf. Sci. 191 (1987) 121.
[37] G.B. Fisher, General Motors Res. Pub. no GMR-4007/PCP-171, 1982.
[38] D.E. Brown, S.M. George, C. Huang, E.K.L. Wong, K.B. Rider, R.S. Smith, B.D. Kay, J. Phys. Chem. 100 (1996) 4988.
[39] J. Liu, M. Xu, T. Nordmeyer, F. Zaera, J. Phys. Chem. 99 (1995) 6167.
[40] H. Ogasawara, J. Yoshinobu, M. Kawai, Surf. Sci. 386 (1997) 73.
[41] P. Lofgren, B. Kasemo, Cat. Lett. 53 (1998) 33.
[42] M. Nakamura, M.B. Song, M. Ito, Chem. Phys. Lett. 320 (2000) 381.
[43] T.E. Madley, J.T. Yates Jr., Chem. Phys. Lett. 51 (1977) 77.
[44] J.P. Devlin, V. Buch, J. Phys. Chem. 99 (1995) 16534.
[45] K. Bolton, J.B.C. Pettersson, J. Phys. Chem. B 104 (2000) 1590.
[46] D. Chakarov, B. Kasemo, Phys. Rev. Lett. 81 (1998) 5181.